Shape optimization of a layer-by-layer constraint functional for additive manufacturing processes

Grégoire Allaire[1], Charles Dapogny[2], Alexis Faure[3], Georgios Michailidis[3], and Rafael Estevez[3]

[1] CMAP, UMR 7641 École Polytechnique, Palaiseau, France
[2] CNRS & Laboratoire Jean Kuntzmann, Université Grenoble-Alpes, Grenoble, France
[3] SiMaP, Université Grenoble-Alpes, Grenoble, France

9th June, 2017

Foreword: shape optimization in the industrial context

- Shape and topology optimization techniques have aroused a tremendous enthusiasm within the engineering and industrial communities.
- One drawback of these methods is that the optimized designs are often too complicated to be constructed by traditional methods such as milling or casting.
- The recent headway made by additive manufacturing methods allow to assemble structures with a high degree of complexity.
- These techniques impose new constraints on the manufactured components.

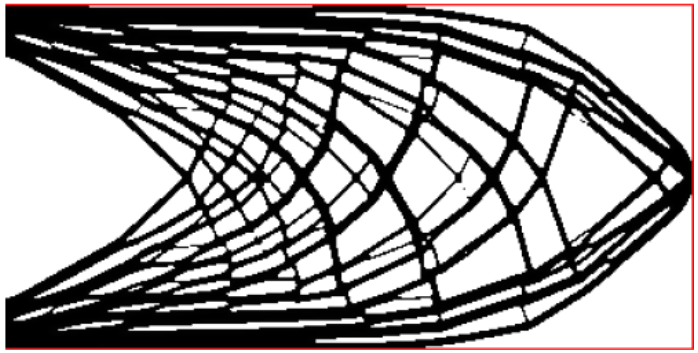

Typical 'truss' designs resulting from shape and topology optimization processes.

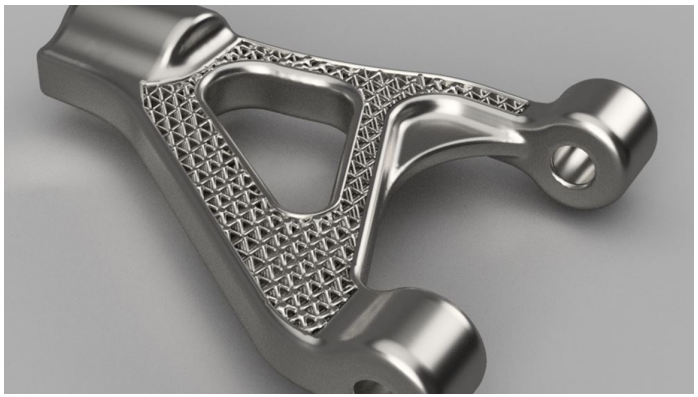

Part produced with an additive manufacturing method (from http://www.autodesk.com/).

1. Additive manufacturing techniques: assets and drawbacks
   - Additive manufacturing in a nutshell
   - The overhang issue
2. The shape optimization problem
3. Geometric constraints for the presence of overhangs
   - The 'naive', geometric attempt
   - Insufficiency of the geometric constraints
4. Geometric constraints for the presence of overhangs
   - Presentation of the mechanical constraint
   - Shape derivative of the mechanical constraint
   - Other models
5. Numerical evaluation of $P_{\mathrm{sw}}(\Omega)$ and its derivative
6. Numerical examples
   - Test of the mechanical approaches
   - Combining the geometric and mechanical approaches

Additive manufacturing in a nutshell (I)

- All the additive manufacturing processes begin with a slicing stage: the input shape is decomposed into a series of horizontal layers.
- These $2d$ layers are built one on top of the other according to the selected technology.

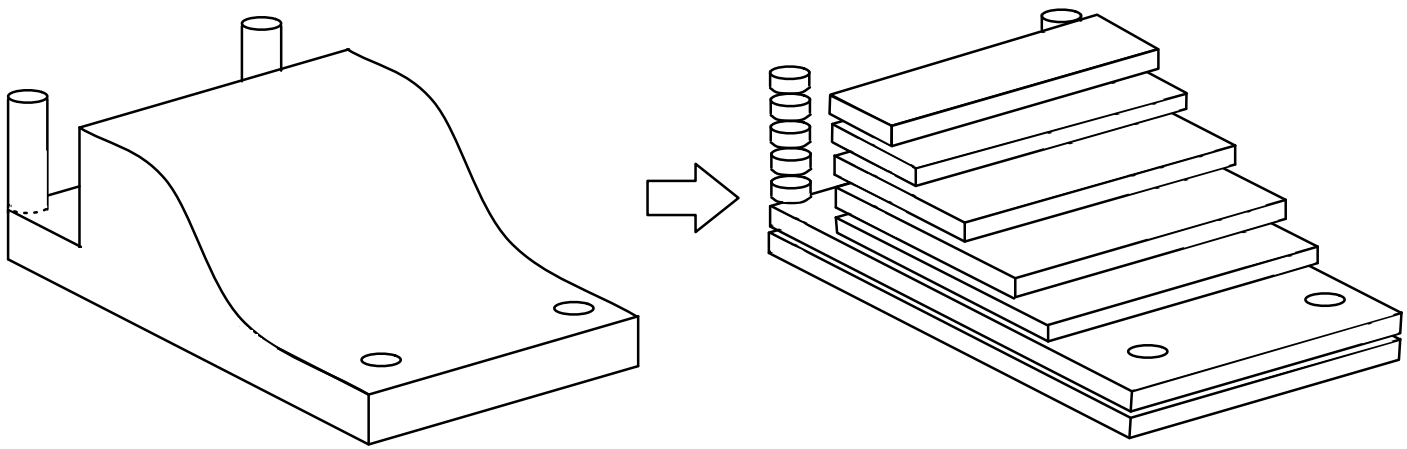

Sketch of the slicing procedure, initiating any additive manufacturing process.

Additive manufacturing in a nutshell (II)

Two popular additive manufacturing technologies are:

- Material extrusion methods (e.g. FDM): they act by direct deposition of rasters of a molten filament. Such methods are often used to process plastic (ABS).
- Powder bed fusion methods (e.g. EBM, SLS), which are generally used to process metals. Each $2d$ layer is assembled by spreading metallic powder within the build chamber, then binding the grains together with a laser.

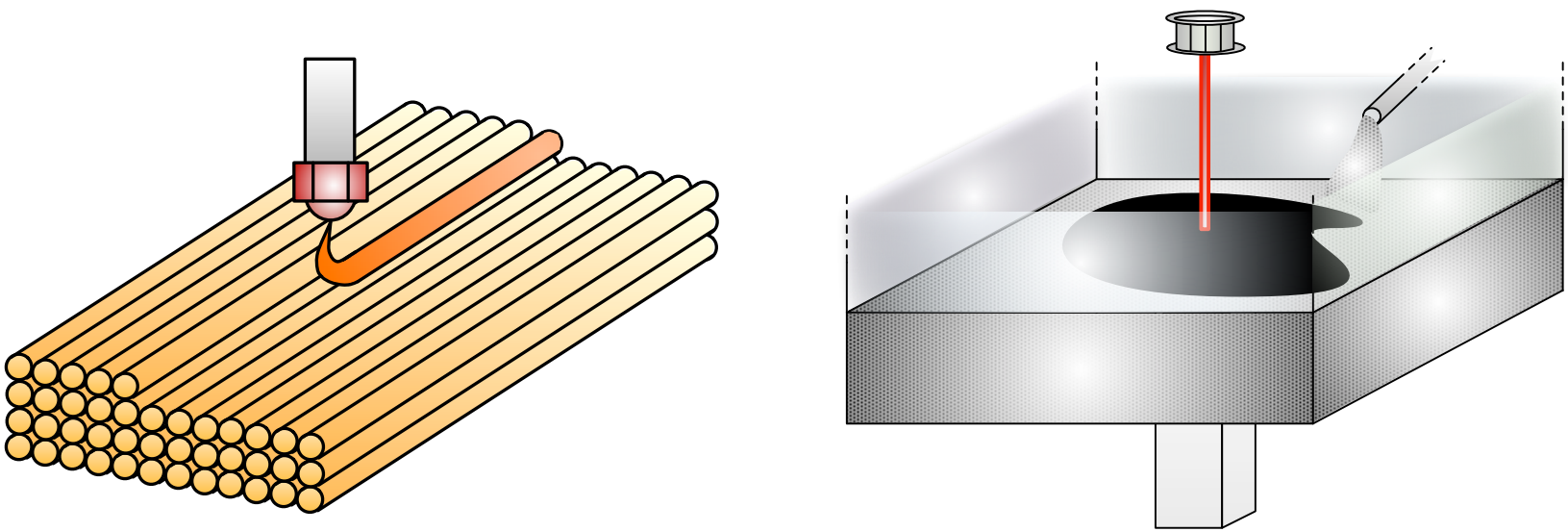

Sketch of the (left) FDM and (right) EBM additive manufacturing processes.

Additive manufacturing techniques in a nutshell (III)

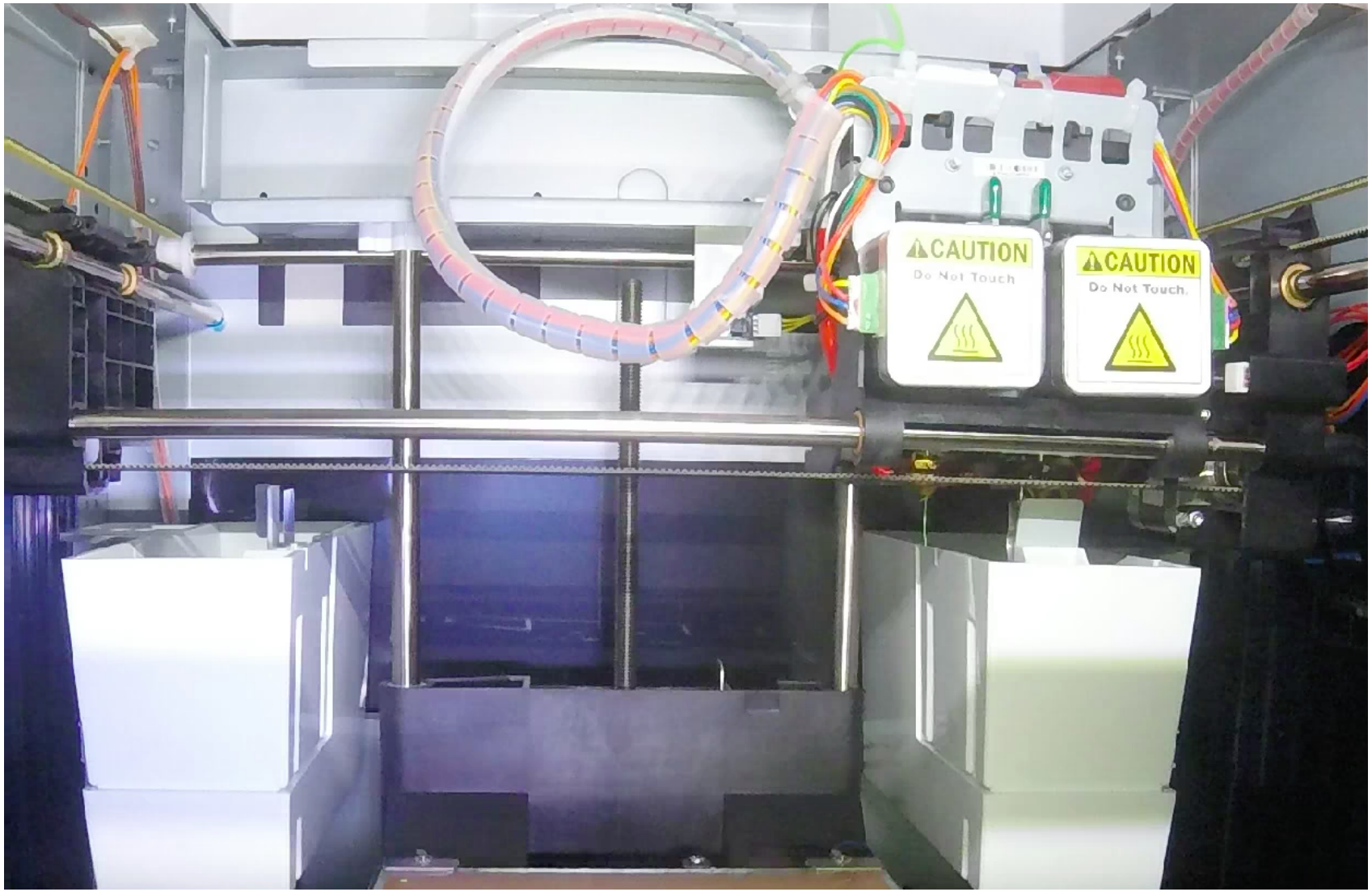

An FDM machine tool in action.

1. Additive manufacturing techniques: assets and drawbacks
   - Additive manufacturing in a nutshell
   - The overhang issue
2. The shape optimization problem
3. Geometric constraints for the presence of overhangs
   - The 'naive', geometric attempt
   - Insufficiency of the geometric constraints
4. Geometric constraints for the presence of overhangs
   - Presentation of the mechanical constraint
   - Shape derivative of the mechanical constraint
   - Other models
5. Numerical evaluation of $P_{\mathrm{sw}}(\Omega)$ and its derivative
6. Numerical examples
   - Test of the mechanical approaches
   - Combining the geometric and mechanical approaches

The overhang issue (I)

All additive manufacturing technologies experience trouble in the assembly of shapes showing large overhangs, i.e. regions hanging over void.

- in the case of FDM processes, this amounts to assembling over void.
- In the case of powder-bed methods, the rapid melting then solidification of the powder induces residual stress, especially in regions unanchored to the lower structure. This may cause warpage of such parts upon cooling.

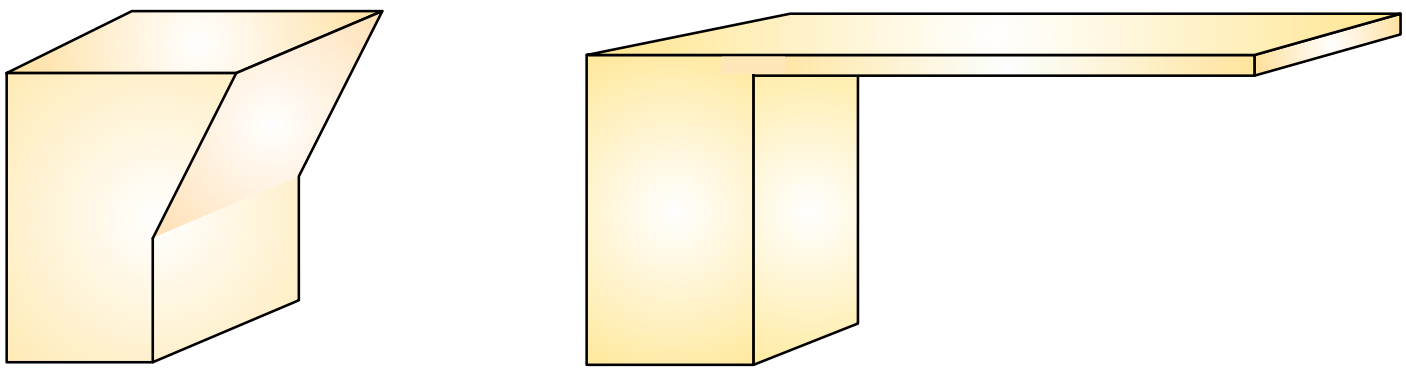

(Left) short overhang; support from the lower structure is sufficient to guarantee manufacturability; (right) large overhang.

The overhang issue (II)

- The most common strategy to deal with overhangs is to erect a sacrificial scaffold structure alongside the construction of the shape [DuHeLe].
- This scaffold structure has to be removed as a post-processing, which is costly and cumbersome.

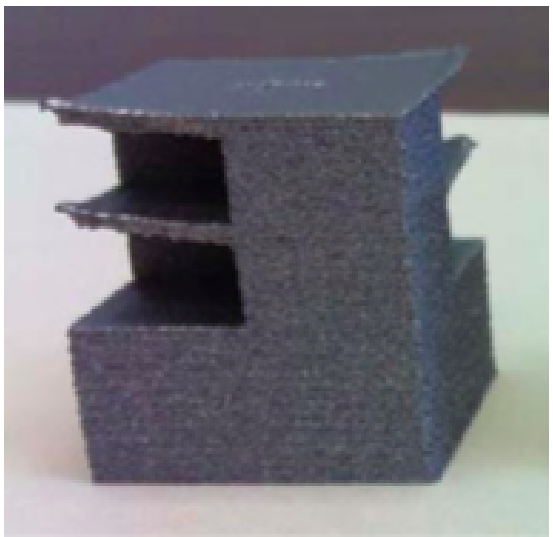

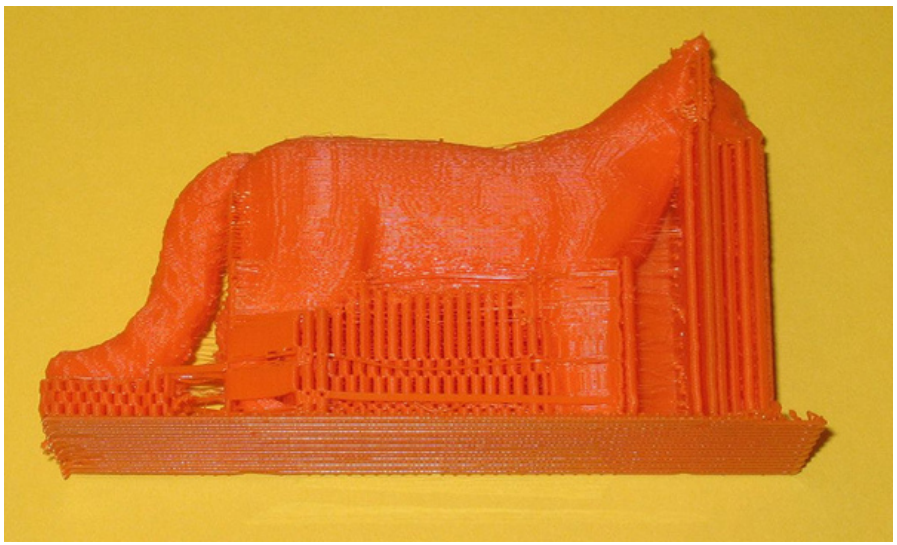

(Left) Warpage caused by residual constraints in an EBM assembly (from [CheLuChou]), (right) scaffold structure in the construction of a part (from `https://hyrulefoundry.wordpress.com/`*).*

1 Additive manufacturing techniques: assets and drawbacks
- Additive manufacturing in a nutshell
- The overhang issue

2 The shape optimization problem

3 Geometric constraints for the presence of overhangs
- The 'naive', geometric attempt
- Insufficiency of the geometric constraints

4 Geometric constraints for the presence of overhangs
- Presentation of the mechanical constraint
- Shape derivative of the mechanical constraint
- Other models

5 Numerical evaluation of $P_{\mathrm{sw}}(\Omega)$ and its derivative

6 Numerical examples
- Test of the mechanical approaches
- Combining the geometric and mechanical approaches

Shape optimization of linear elastic shapes (I)

In the context of its final use, a shape is a bounded domain $\Omega \subset \mathbb{R}^d$, which is

- fixed on a part Γ_D of its boundary,
- submitted to surface loads f, applied on $\Gamma_N \subset \partial\Omega$, $\Gamma_D \cap \Gamma_N = \emptyset$.

The displacement vector field $u_\Omega : \Omega \to \mathbb{R}^d$ is governed by the linear elasticity system:

$$\left\{ \begin{array}{rcll} -\mathrm{div}(Ae(u_\Omega)) & = & 0 & \text{in } \Omega \\ u_\Omega & = & 0 & \text{on } \Gamma_D \\ Ae(u_\Omega)n & = & f & \text{on } \Gamma_N \\ Ae(u_\Omega)n & = & 0 & \text{on } \Gamma \end{array} \right. ,$$

where $e(u) = \frac{1}{2}(\nabla u^T + \nabla u)$ is the strain tensor, and A is the Hooke's law of the material:

$$\forall e \in \mathcal{S}_d(\mathbb{R}), \quad Ae = 2\mu e + \lambda \mathrm{tr}(e) I.$$

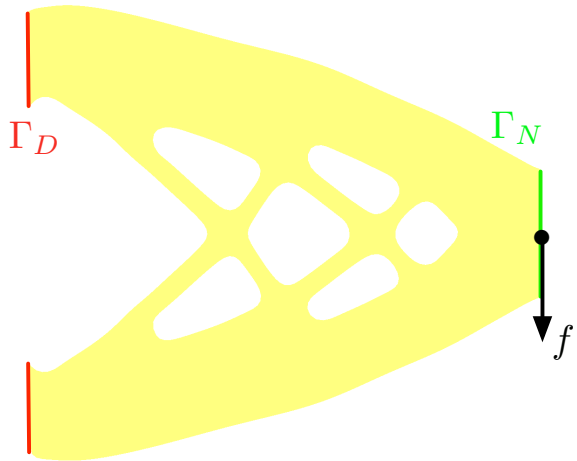

A 'Cantilever'

The deformed cantilever

The shape optimization problem

The shape optimization problem of interest reads:

$$\min_{\mathcal{U}_{\mathrm{ad}}} J(\Omega), \text{ s.t. } P(\Omega) \leq \alpha,$$

in which

- $\mathcal{U}_{\mathrm{ad}}$ is a set of (smooth) admissible shapes,
- The objective function $J(\Omega)$ is the structural compliance of shapes:

$$J(\Omega) = \int_{\Omega} Ae(u_\Omega) : e(u_\Omega)\, dx = \int_{\Gamma_N} f \cdot u_\Omega\, ds,$$

- The constraint $P(\Omega)$ enforces the constructibility by additive manufacturing processes,
- Other constraints may be added to the problem, e.g. on the volume $\mathrm{Vol}(\Omega)$ of shapes.

Differentiation with respect to the domain: Hadamard's method

Hadamard's boundary variation method describes variations of a reference, Lipschitz domain Ω of the form:

$$\Omega \to \Omega_\theta := (\mathrm{Id} + \theta)(\Omega),$$

for 'small' $\theta \in W^{1,\infty}\left(\mathbb{R}^d, \mathbb{R}^d\right)$.

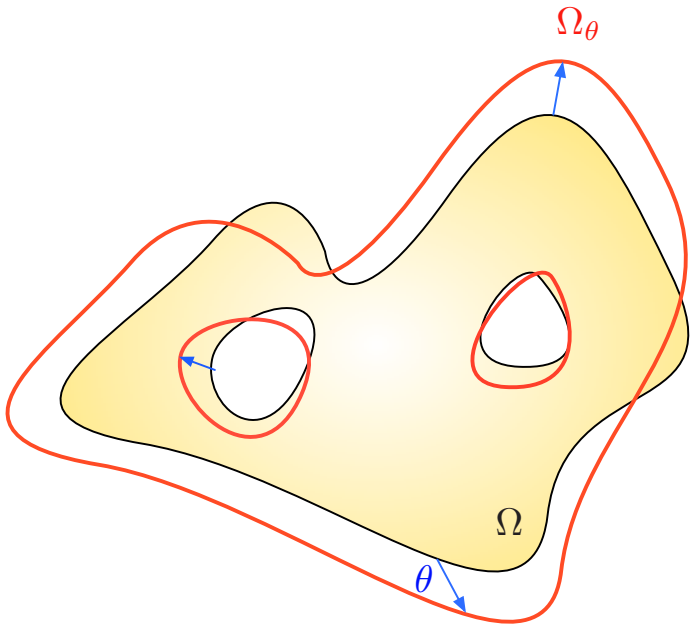

Definition 1.

Given a smooth domain Ω, a function $J(\Omega)$ of the domain is shape differentiable at Ω if the function

$$W^{1,\infty}(\mathbb{R}^d, \mathbb{R}^d) \ni \theta \mapsto J(\Omega_\theta)$$

is Fréchet-differentiable at 0, i.e. the following expansion holds around 0:

$$J(\Omega_\theta) = J(\Omega) + J'(\Omega)(\theta) + o\left(||\theta||_{W^{1,\infty}(\mathbb{R}^d,\mathbb{R}^d)}\right).$$

Differentiation with respect to the domain: Hadamard's method

Techniques from optimal control theory make it possible to calculate shape derivatives; in the case of 'many' functionals of the domain $J(\Omega)$, the shape derivative has the particular structure:

$$J'(\Omega)(\theta) = \int_\Gamma v_\Omega \, \theta \cdot n \, ds,$$

where v_Ω is a scalar field depending on u_Ω, and possibly on an adjoint state p_Ω.

Example: If the objective function

$$J(\Omega) = \int_{\Gamma_N} f \cdot u_\Omega \, ds$$

is the compliance, $v_\Omega = -Ae(u_\Omega) : e(u_\Omega)$ is the (negative) elastic energy density.

The generic algorithm

This shape gradient provides a natural descent direction for $J(\Omega)$: *for instance*, defining θ as

$$\theta = -v_\Omega n$$

yields, for $t > 0$ sufficiently small (*to be found numerically*):

$$J((\mathrm{Id} + t\theta)(\Omega)) = J(\Omega) - t\int_\Gamma v_\Omega^2 ds + o(t) < J(\Omega)$$

Gradient algorithm: For $n = 0, \ldots$ until convergence,

1. Compute the solution u_{Ω^n} (and p_{Ω^n}) of the elasticity system on Ω^n.
2. Compute the shape gradient $J'(\Omega^n)$ thanks to the previous formula, and infer a descent direction θ^n for the cost functional.
3. Advect the shape Ω^n according to θ^n, so as to get $\Omega^{n+1} := (\mathrm{Id} + \theta^n)(\Omega^n)$.

1 Additive manufacturing techniques: assets and drawbacks
- Additive manufacturing in a nutshell
- The overhang issue

2 The shape optimization problem

3 Geometric constraints for the presence of overhangs
- The 'naive', geometric attempt
- Insufficiency of the geometric constraints

4 Geometric constraints for the presence of overhangs
- Presentation of the mechanical constraint
- Shape derivative of the mechanical constraint
- Other models

5 Numerical evaluation of $P_{\mathrm{sw}}(\Omega)$ and its derivative

6 Numerical examples
- Test of the mechanical approaches
- Combining the geometric and mechanical approaches

The 'naive', geometric attempt (I)

- Most approaches in the literature rely on the angle between $\partial\Omega$ and the (vertical) build direction to detect and penalize overhangs.
- An intuitive approach relies on anisotropic perimeter functionals of the form:

$$P_g(\Omega) = \int_{\partial\Omega} \varphi(n_\Omega)\, ds, \text{ where } \varphi : \mathbb{R}^d \to \mathbb{R} \text{ is given.}$$

Example The choice $\varphi_a(n) := (n \cdot e_d + \cos\nu)_-^2$, where $(s)_- := \min(s, 0)$, penalizes regions of $\partial\Omega$ where the angle $n \cdot (-e_d)$ is smaller than a threshold ν.

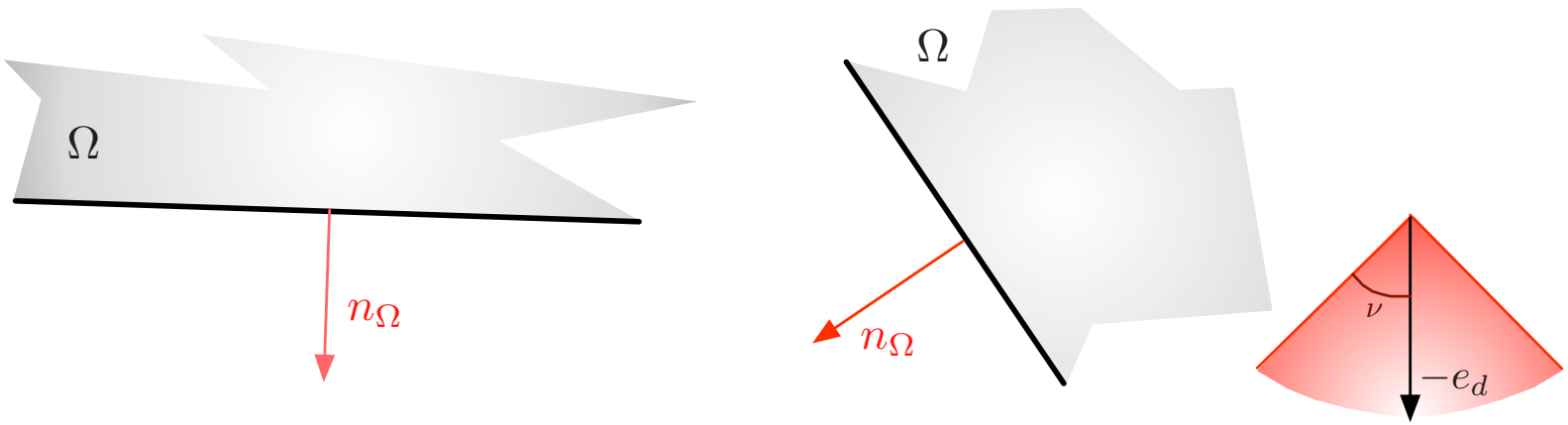

Parts of $\partial\Omega$ (left) violating and (right) satisfying the angle-based criterion.

The 'naive', geometric attempt (II)

Proposition 1.

The functional $P_g(\Omega)$ is shape differentiable at any admissible shape $\Omega \in \mathcal{U}_{\mathrm{ad}}$, and its shape derivative reads:

$$P_g'(\Omega)(\theta) = \int_\Gamma \kappa\, \varphi(n)\, \theta \cdot n \, ds - \int_\Gamma \nabla(\varphi(n)) \cdot \nabla_{\partial\Omega}(\theta \cdot n)\, ds,$$

where $\nabla_{\partial\Omega}\psi := \nabla\psi - (\nabla\psi \cdot n)n$ is the tangential gradient of a smooth enough function $\psi : \partial\Omega \to \mathbb{R}$.

- Unfortunately, this approach gives unsatisfactory results.
- We propose instead a general idea for modeling overhang constraints, which appeals to their mechanical origin.

1 Additive manufacturing techniques: assets and drawbacks
- Additive manufacturing in a nutshell
- The overhang issue

2 The shape optimization problem

3 Geometric constraints for the presence of overhangs
- The 'naive', geometric attempt
- Insufficiency of the geometric constraints

4 Geometric constraints for the presence of overhangs
- Presentation of the mechanical constraint
- Shape derivative of the mechanical constraint
- Other models

5 Numerical evaluation of $P_{\mathrm{sw}}(\Omega)$ and its derivative

6 Numerical examples
- Test of the mechanical approaches
- Combining the geometric and mechanical approaches

Geometric constraints; the 'dripping effect' (I)

We consider the two-dimensional MBB Beam example.

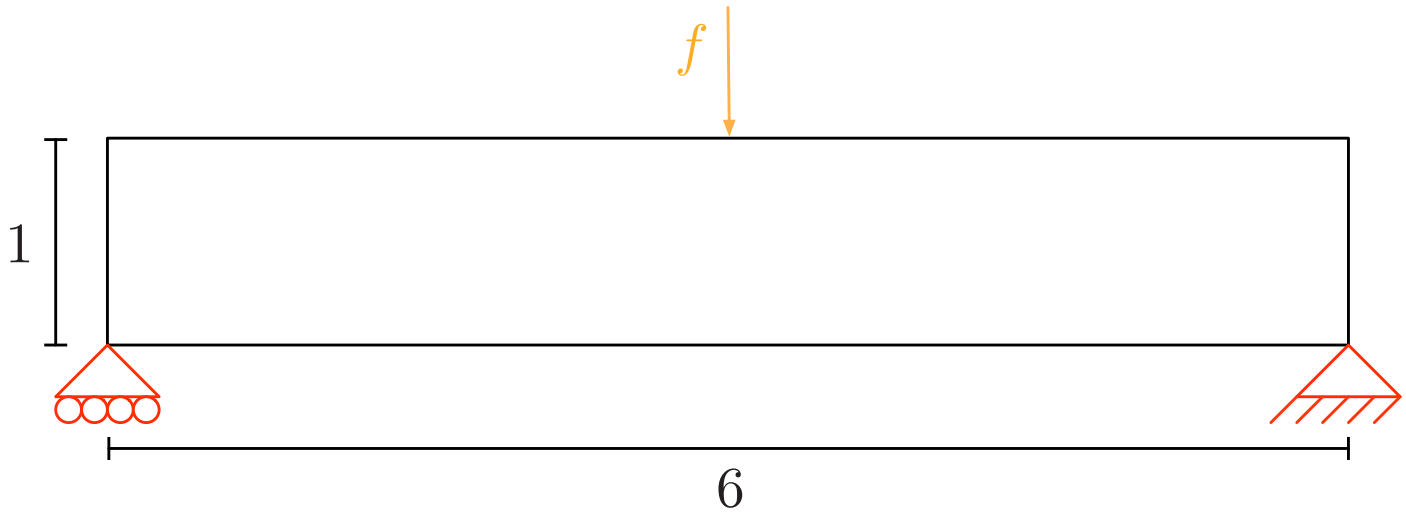

Setting of the two-dimensional MBB beam example.

We first solve the compliance minimization problem:

$$\begin{aligned} \min_{\Omega} \quad & J(\Omega), \\ \text{s.t.} \quad & \mathrm{Vol}(\Omega) \leq \alpha_v \mathrm{Vol}(D). \end{aligned}$$

Geometric constraints; the 'dripping effect' (II)

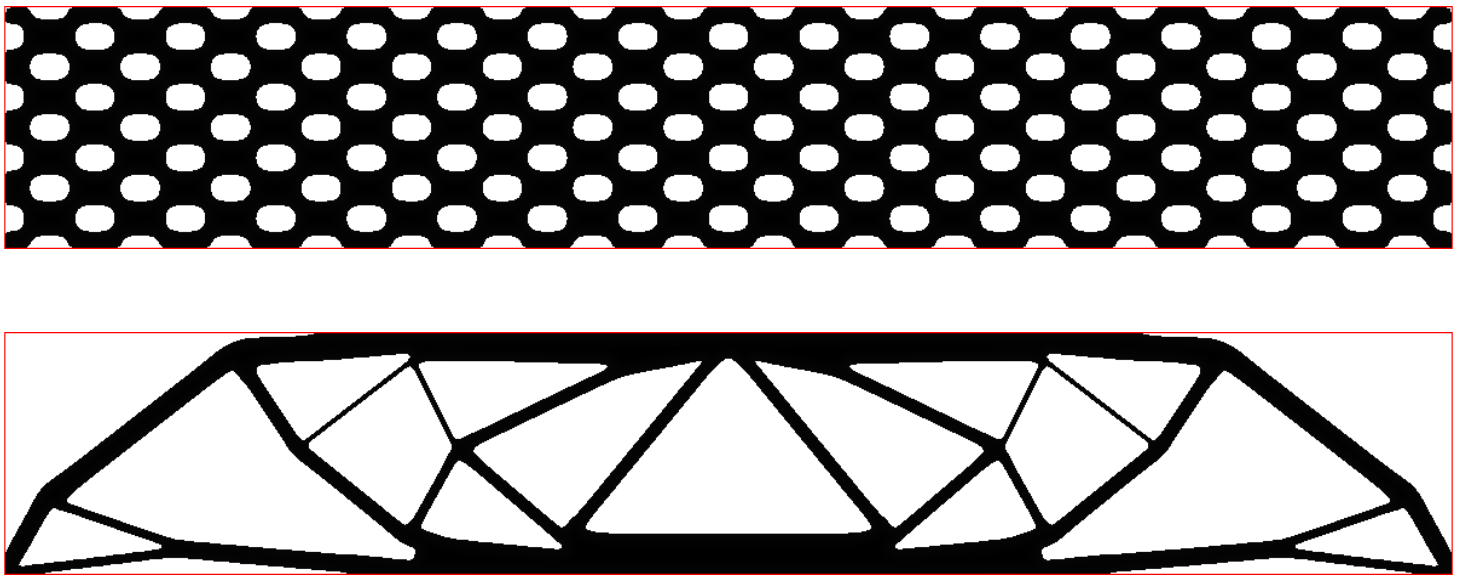

(Top) initial shape Ω_0 and (bottom) optimized shape Ω^* for compliance minimization in the two-dimensional MBB Beam example.

The optimized shape Ω^* presents large nearly horizontal bars which are very important for the structural performance.

Geometric constraints; the 'dripping effect' (III)

To help in removing these overhangs, we rather solve the problem:

$$\begin{array}{ll} \min\limits_{\Omega} & (1-\alpha_g)\frac{J(\Omega)}{J(\Omega^*)} + \alpha_g \frac{P_g(\Omega)}{P_g(\Omega^*)}, \\ \text{s.t.} & \mathrm{Vol}(\Omega) \leq \alpha_v \mathrm{Vol}(D). \end{array}$$

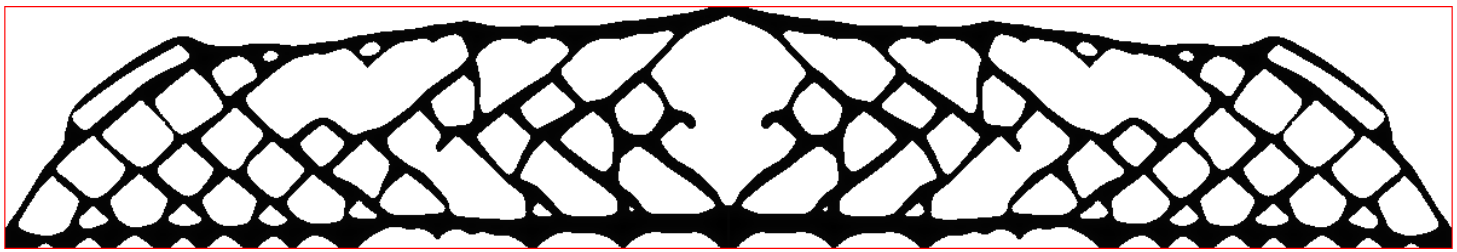

Optimized shape using $\alpha_g = 0.5$.

The shape develops an oscillatory boundary so that:

- The angle requirement is (approximately) satisfied,
- The structural performance is not too much altered: the large bars connecting loads to anchor points have not disappeared.

Geometric constraints; the 'dripping effect' (IV)

Adding a perimeter constraint to the problem is a tentative remedy, but does not prove sufficient to deal with this issue.

Optimized shape using angle and perimeter penalization.

1 Additive manufacturing techniques: assets and drawbacks
- Additive manufacturing in a nutshell
- The overhang issue

2 The shape optimization problem

3 Geometric constraints for the presence of overhangs
- The 'naive', geometric attempt
- Insufficiency of the geometric constraints

4 Geometric constraints for the presence of overhangs
- Presentation of the mechanical constraint
- Shape derivative of the mechanical constraint
- Other models

5 Numerical evaluation of $P_{\mathrm{sw}}(\Omega)$ and its derivative

6 Numerical examples
- Test of the mechanical approaches
- Combining the geometric and mechanical approaches

Definition of the mechanical constraint (I)

The mechanical constraint $P(\Omega)$ relies on the physical behavior of the shape at each stage of its construction.

- Ω is enclosed in the build chamber $D = S \times (0, H)$, where $S \subset \mathbb{R}^{d-1}$,
- $\Omega_h := \{x = (x_1, ..., x_d) \in \Omega,\ x_d < h\}$ is the intermediate shape at height h.
- The boundary $\partial\Omega_h$ is decomposed as $\partial\Omega_h = \Gamma_0 \cup \Gamma_h^u \cup \Gamma_h^l$, where
  - $\Gamma_0 = \{x \in \partial\Omega_h,\ x_d = 0\}$ is the contact region between Ω and the build table,
  - $\Gamma_h^u = \{x \in \partial\Omega_h,\ x_d = h\}$ is the upper side of Ω_h,
  - $\Gamma_h^l = \partial\Omega_h \setminus (\overline{\Gamma_0} \cup \overline{\Gamma_h^u})$ is the lateral surface.

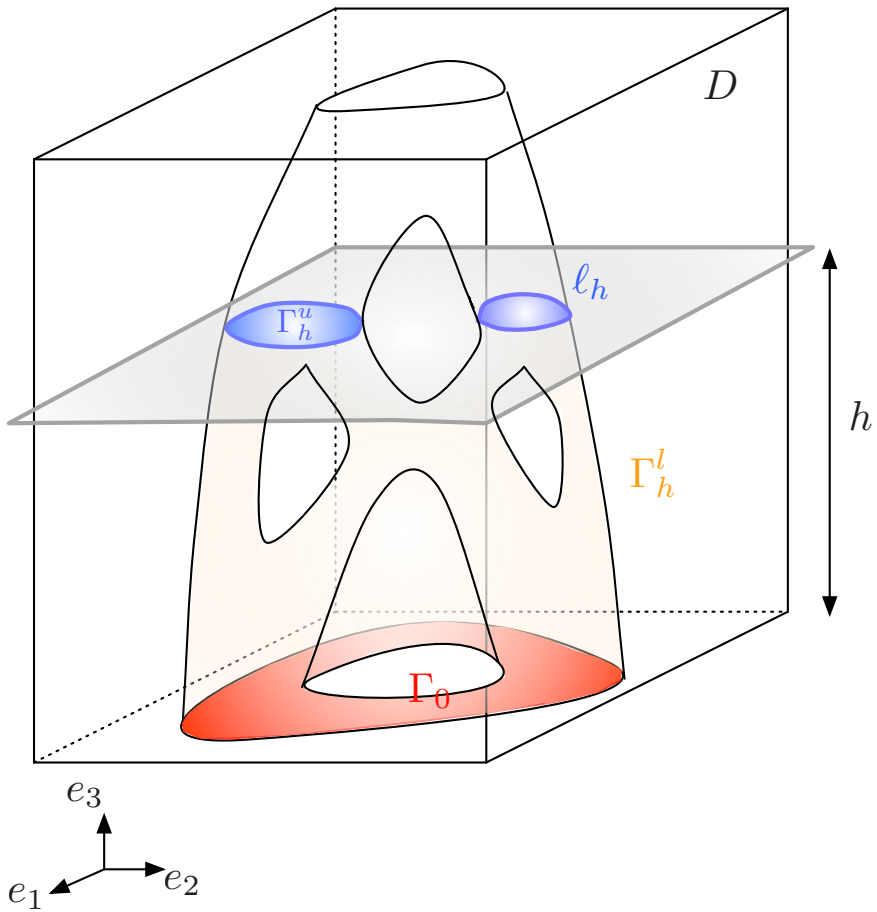

Definition of the mechanical constraint (II)

- Each intermediate shape Ω_h is only subjected to gravity effects $g \in H^1(\mathbb{R}^d)^d$. The elastic displacement of Ω_h satisfies:

$$\begin{cases} -\mathrm{div}(Ae(u^c_{\Omega_h})) = g & \text{in } \Omega_h, \\ u^c_{\Omega_h} = 0 & \text{on } \Gamma_0, \\ Ae(u^c_{\Omega_h})n = 0 & \text{on } \Gamma^l_h \cup \Gamma^u_h. \end{cases}$$

- The self-weight of each intermediate shape Ω_h is:

$$c_{\Omega_h} := \int_{\Omega_h} Ae(u^c_{\Omega_h}) : e(u^c_{\Omega_h})\, dx = \int_{\Omega_h} g \cdot u^c_{\Omega_h}\, dx.$$

- The (self-weight) manufacturing compliance of a final shape Ω aggregates the self weights of all its intermediate shapes:

$$P_{\mathrm{sw}}(\Omega) = \int_0^H j(c_{\Omega_h})\, dh,$$

where $j : \mathbb{R} \to \mathbb{R}$ is a smooth function.

1 Additive manufacturing techniques: assets and drawbacks
- Additive manufacturing in a nutshell
- The overhang issue

2 The shape optimization problem

3 Geometric constraints for the presence of overhangs
- The 'naive', geometric attempt
- Insufficiency of the geometric constraints

4 Geometric constraints for the presence of overhangs
- Presentation of the mechanical constraint
- Shape derivative of the mechanical constraint
- Other models

5 Numerical evaluation of $P_{\mathrm{sw}}(\Omega)$ and its derivative

6 Numerical examples
- Test of the mechanical approaches
- Combining the geometric and mechanical approaches

Shape derivative of the manufacturing compliance (I)

- We consider a fixed shape $\Omega \in \mathcal{U}_{\mathrm{ad}}$.
- Perturbations θ are confined to a class X^k of vector fields of class $\mathcal{C}^k$, which identically vanish near the 'flat regions' of $\partial\Omega$.

Theorem 2.

The manufacturing compliance $P_{\mathrm{sw}}(\Omega)$ is shape differentiable at Ω, in the sense that the mapping $\theta \mapsto P_{\mathrm{sw}}(\Omega_\theta)$, from X^k into $\mathbb{R}$ is differentiable for $k \geq 1$. Its derivative is:

$$\forall \theta \in X^k, \quad P'_{\mathrm{sw}}(\Omega)(\theta) = \int_{\partial\Omega \setminus \overline{\Gamma_0}} \mathcal{D}_\Omega \, \theta \cdot n \, ds,$$

where the integrand factor $\mathcal{D}_\Omega$ is defined, for a.e. $x \in \partial\Omega \setminus \overline{\Gamma_0}$, by:

$$\mathcal{D}_\Omega(x) = \int_{x_d}^{H} j'(c_{\Omega_h}) \left(2g \cdot u^c_{\Omega_h} - Ae(u^c_{\Omega_h}) : e(u^c_{\Omega_h})\right)(x) \, dh.$$

Shape derivative of the mechanical constraint (II)

Sketch of the proof: The proof is not completely standard since cuts $(\Omega_\theta)_h$ of variations of Ω are not 'classical' variations of shapes.

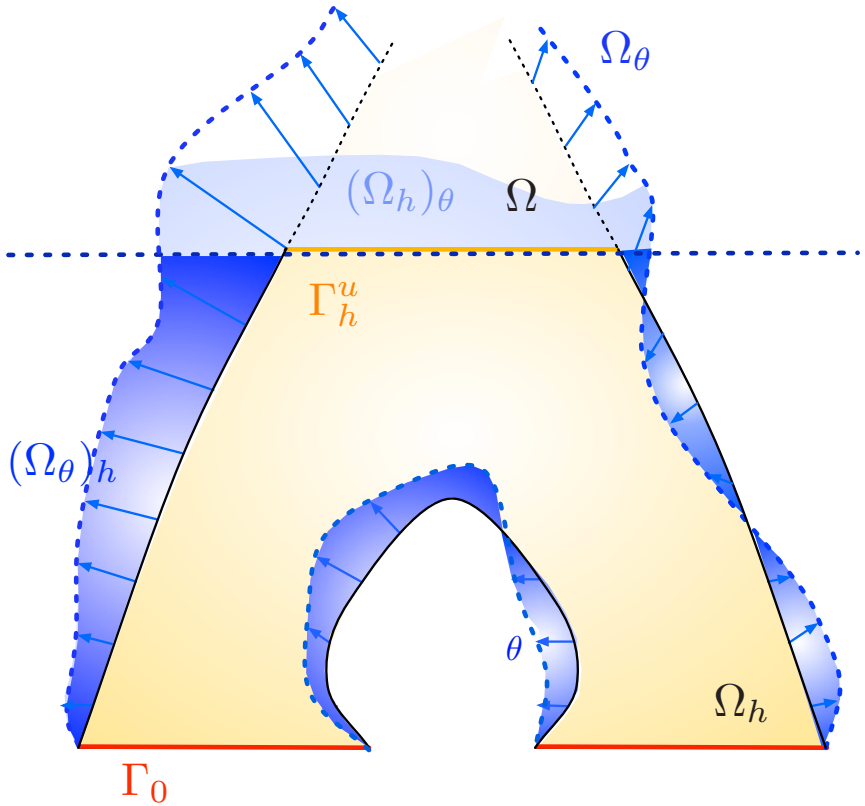

In general, cuts $(\Omega_\theta)_h$ cannot be described as variations (e.g. $(\Omega_h)_\theta$) of Ω_h.

Step I: The case of horizontal perturbations

Step 1 The Theorem holds in the particular case of horizontal perturbations

$$\theta \in X_H^k, \;\; X_H^k := \left\{ \theta \in X^k, \; \theta \cdot e_d = 0 \right\}.$$

This part boils down to classical variations of shape, since in this case:

$$(\Omega_\theta)_h = (\Omega_h)_\theta.$$

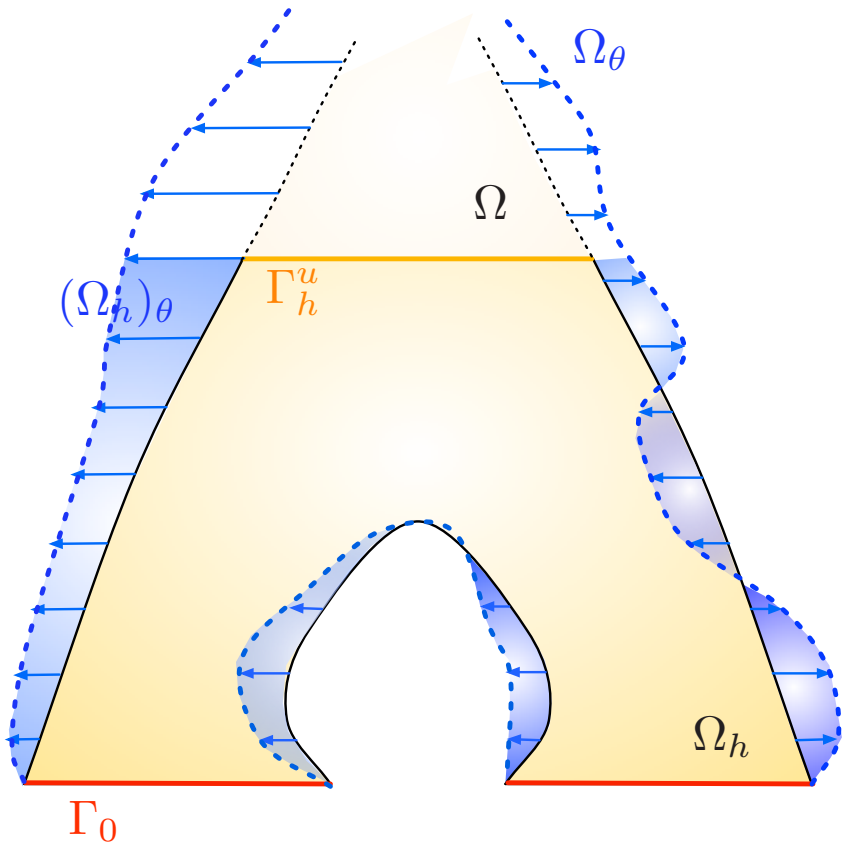

Step II: From 'general' to horizontal perturbations

Step 2 We prove that every variation Ω_θ of Ω with $\theta \in X^{k+1}$ can be described under the form $\Omega_{\xi(\theta)}$, where $\xi(\theta) \in X^k_H$ is horizontal.

We also calculate the derivative of the mapping $\theta \mapsto \xi(\theta)$.

This is an application of the implicit function theorem, upon rewriting an equality such as $\Omega_\theta = \Omega_\xi$ under the form

$$\mathcal{G}(\theta, \xi) = 0.$$

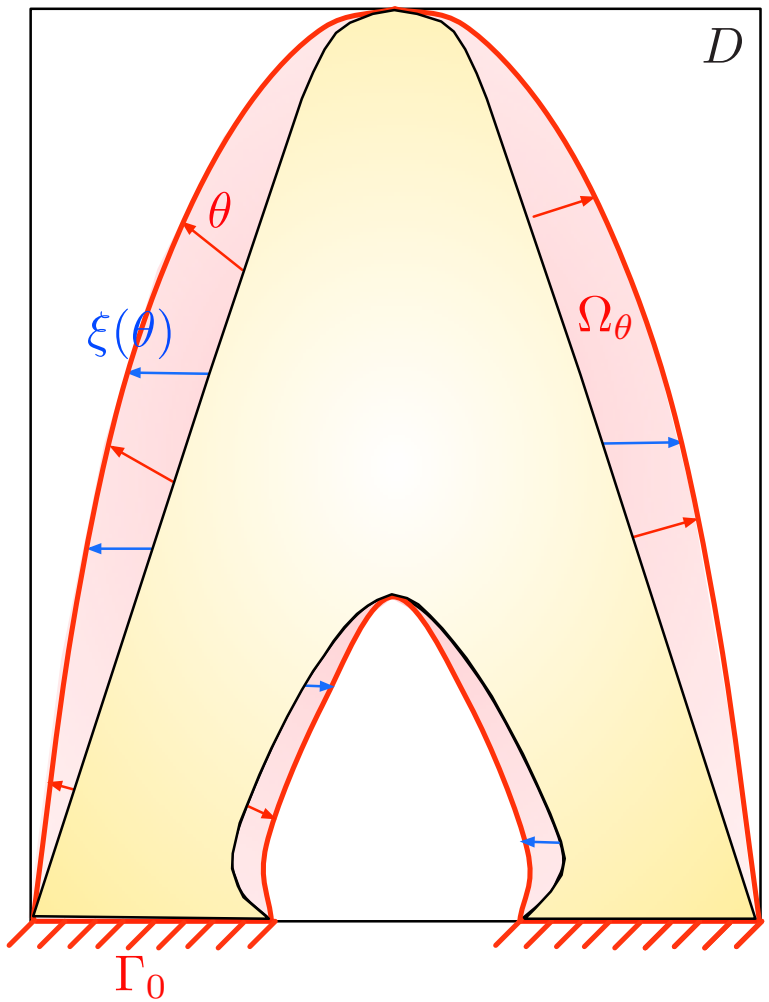

Step III: Use of the chain rule

Step III The differentiability of

$$\theta \mapsto P_{\mathrm{sw}}(\Omega_\theta) = P_{\mathrm{sw}}((\Omega_{\xi(\theta)})$$

follows from the chain rule.

□

1 Additive manufacturing techniques: assets and drawbacks
- Additive manufacturing in a nutshell
- The overhang issue

2 The shape optimization problem

3 Geometric constraints for the presence of overhangs
- The 'naive', geometric attempt
- Insufficiency of the geometric constraints

4 Geometric constraints for the presence of overhangs
- Presentation of the mechanical constraint
- Shape derivative of the mechanical constraint
- Other models

5 Numerical evaluation of $P_{\mathrm{sw}}(\Omega)$ and its derivative

6 Numerical examples
- Test of the mechanical approaches
- Combining the geometric and mechanical approaches

Other models

Other models may be used for the physical behavior of intermediate shapes Ω_h. For instance,

- The definition of $u^c_{\Omega_h}$ could be replaced by:

$$\begin{cases} -\mathrm{div}(Ae(u^a_{\Omega_h})) = g_h & \text{in } \Omega_h, \\ u^a_{\Omega_h} = 0 & \text{on } \Gamma_0, \\ Ae(u^a_{\Omega_h})n = 0 & \text{on } \Gamma^l_h, \\ Ae(u^a_{\Omega_h})n = 0 & \text{on } \Gamma^u_h, \end{cases} \quad \text{where } g_h(x) = \begin{cases} g & \text{if } x_d \in (h-\delta, h), \\ 0 & \text{otherwise,} \end{cases}$$

  is an artificial force acting on the upper side of Ω_h. As we shall see, this formulation is better at penalizing perfectly horizontal parts hanging over void.

- The mechanical constraint $P(\Omega)$ could involve the solutions v_{Ω_h} to a thermal cooling problem posed on Ω_h, to model e.g. residual stresses in the final shape Ω; see [AlJak].

1 Additive manufacturing techniques: assets and drawbacks
- Additive manufacturing in a nutshell
- The overhang issue

2 The shape optimization problem

3 Geometric constraints for the presence of overhangs
- The 'naive', geometric attempt
- Insufficiency of the geometric constraints

4 Geometric constraints for the presence of overhangs
- Presentation of the mechanical constraint
- Shape derivative of the mechanical constraint
- Other models

5 Numerical evaluation of $P_{\mathrm{sw}}(\Omega)$ and its derivative

6 Numerical examples
- Test of the mechanical approaches
- Combining the geometric and mechanical approaches

Numerical evaluation of $P_{\mathrm{sw}}(\Omega)$ and $P'_{\mathrm{sw}}(\Omega)(\theta)$

- The expressions for $P_{\mathrm{sw}}(\Omega)$ and its derivative $P'_{\mathrm{sw}}(\Omega)(\theta)$

$$P_{\mathrm{sw}}(\Omega) = \int_0^H j(c_{\Omega_h})\, dh, \text{ and } P'_{\mathrm{sw}}(\Omega)(\theta) = \int_{\partial\Omega\setminus\overline{\Gamma_0}} \mathcal{D}_\Omega\, \theta\cdot n\, ds,$$

where

$$\mathcal{D}_\Omega(x) = \int_{x_d}^H j'(c_{\Omega_h})\left(2g\cdot u^c_{\Omega_h} - Ae(u^c_{\Omega_h}) : e(u^c_{\Omega_h})\right)(x)\, dh.$$

involve a continuum of shapes Ω_h via the self-weights c_{Ω_h} and the elastic displacements $u^c_{\Omega_h}$,

- Hence the need for a suitable discretization of $h \mapsto c_{\Omega_h}$ and $h \mapsto u^c_{\Omega_h}$.
- We present:
  - 0^{th}-order approximations P^0_N and $\mathcal{D}^0_N$ of $P_{\mathrm{sw}}(\Omega)$ and $\mathcal{D}_\Omega$,
  - First-order approximations P^1_N and $\mathcal{D}^1_N$ based on an interpolation procedure.

The 'naive', 0^{th} order method

- The height interval $(0, H)$ is discretized with a sequence:

$$0 < h_1 < h_2 < \ldots < h_N = H.$$

- On each interval $I_i := (h_i, h_{i+1})$, we approximate $h \mapsto c_{\Omega_h}$ and $h \mapsto u^c_{\Omega_h}$ by constant quantities:

$$c_{\Omega_h} \approx c_{\Omega_{h_{i+1}}}, \text{ and } u^c_{\Omega_h} \approx u^c_{\Omega_{h_{i+1}}} \text{ on } \Omega_h, \text{ for } h \in (h_i, h_{i+1}).$$

- These approximations are used in the formulas for $P_{\text{sw}}(\Omega)$ and $P'_{\text{sw}}(\Omega)(\theta)$ to obtain the reconstructions P^0_N and $\mathcal{D}^0_N$.

- This method is costly in practice, since it requires a fine discretization $\{h_i\}$ of $(0, H)$ to be accurate enough.

A first-order interpolation method (I)

- On each interval I_i, we approximate $h \mapsto c_{\Omega_h}$ by a cubic spline $h \mapsto \widetilde{c}_i(h)$ by using the data:

$$\widetilde{c}_i(h_i) = c_{\Omega_{h_i}}, \quad \widetilde{c}_i(h_{i+1}) = c_{\Omega_{h_{i+1}}}, \quad \widetilde{c}_i{}'(h_i) = \left.\frac{d}{dh}(c_{\Omega_h})\right|_{h_i},$$

$$\text{and } \widetilde{c}_i{}'(h_{i+1}) = \left.\frac{d}{dh}(c_{\Omega_h})\right|_{h_{i+1}}.$$

- On each interval I_i, we approximate $h \mapsto u^c_{\Omega_h}$ by:

$$u^c_{\Omega_h} \approx u^c_{\Omega_{h_{i+1}}}(x) + (h_{i+1} - h)\, U_{\Omega_{h_{i+1}}}(x), \text{ a.e. } x \in \Omega_h,$$

where U_{Ω_h} is the 'derivative' of the mapping $h \mapsto u^c_{\Omega_h}$... in a suitable sense.

- These quantities are used in the definitions of $P_{\mathrm{sw}}(\Omega)$ and $P'_{\mathrm{sw}}(\Omega)(\theta)$ to obtain the approximations P^1_N and $\mathcal{D}^1_N$.

A first-order interpolation method (II)

The derivative of $h \mapsto u^c_{\Omega_h}$ may be thought of as the shape (or Eulerian) derivative of the mapping $t \mapsto u^c_{T_t(\Omega_h)}$, where $T_t : \Omega_h \to \Omega_{h-t}$ is 'any' diffeomorphism from Ω_h onto Ω_{h-t}.

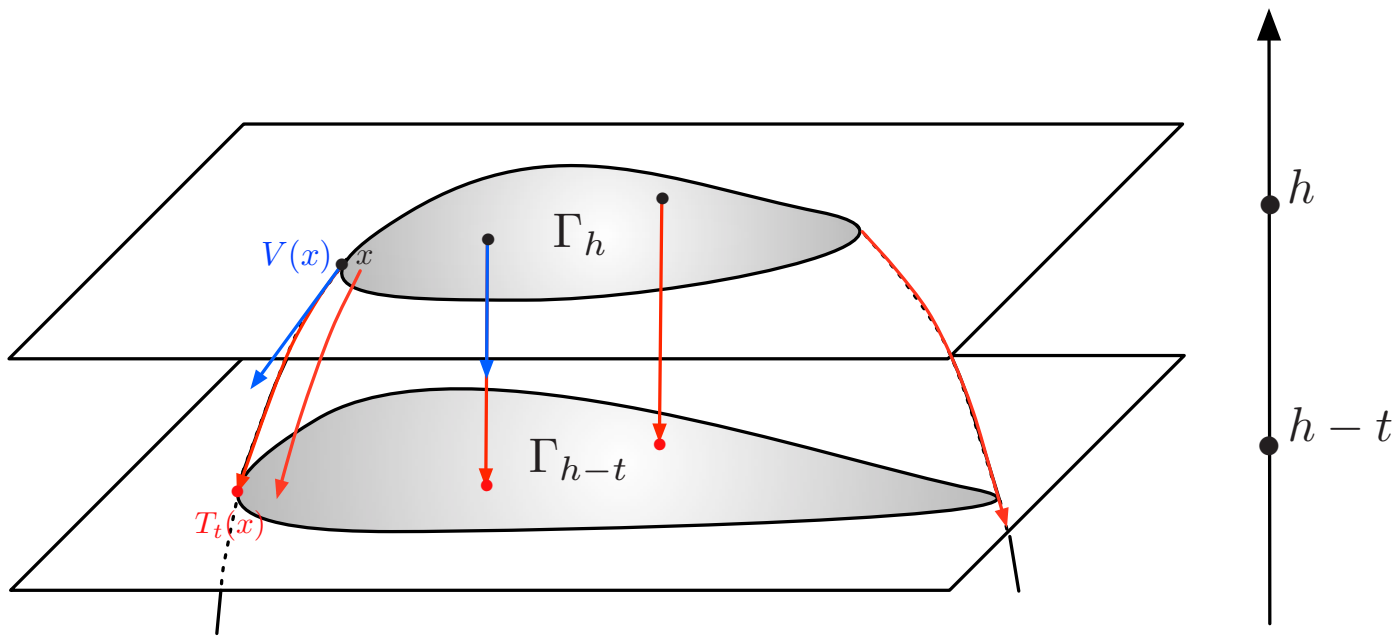

One diffeomorphism T_t mapping Ω_h onto Ω_{h-t}.

1. Additive manufacturing techniques: assets and drawbacks
   - Additive manufacturing in a nutshell
   - The overhang issue
2. The shape optimization problem
3. Geometric constraints for the presence of overhangs
   - The 'naive', geometric attempt
   - Insufficiency of the geometric constraints
4. Geometric constraints for the presence of overhangs
   - Presentation of the mechanical constraint
   - Shape derivative of the mechanical constraint
   - Other models
5. Numerical evaluation of $P_{\mathrm{sw}}(\Omega)$ and its derivative
6. Numerical examples
   - Test of the mechanical approaches
   - Combining the geometric and mechanical approaches

Mechanical approach: the manufacturing compliance (I)

Still in the setting of the two-dimensional MBB Beam example,

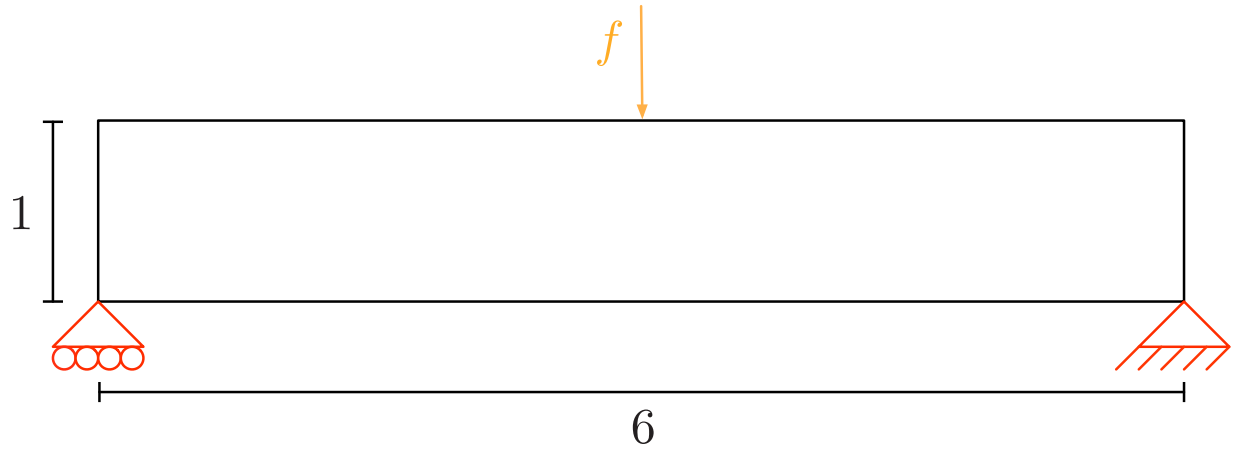

we now solve the constrained optimization problem:

$$\begin{aligned} \min_{\Omega} \quad & J(\Omega) \\ \text{s.t.} \quad & \mathrm{Vol}(\Omega) \leq \alpha_v \mathrm{Vol}(D), \\ & P_{\mathrm{sw}}(\Omega) \leq \alpha_c P_{\mathrm{sw}}(\Omega^*), \end{aligned}$$

where $\alpha_c \in [0, 1]$ is a user-defined tolerance, and Ω^* is the optimized shape for the compliance under volume constraint (without additive manufacturing constraint).

Mechanical approach: the manufacturing compliance (II)

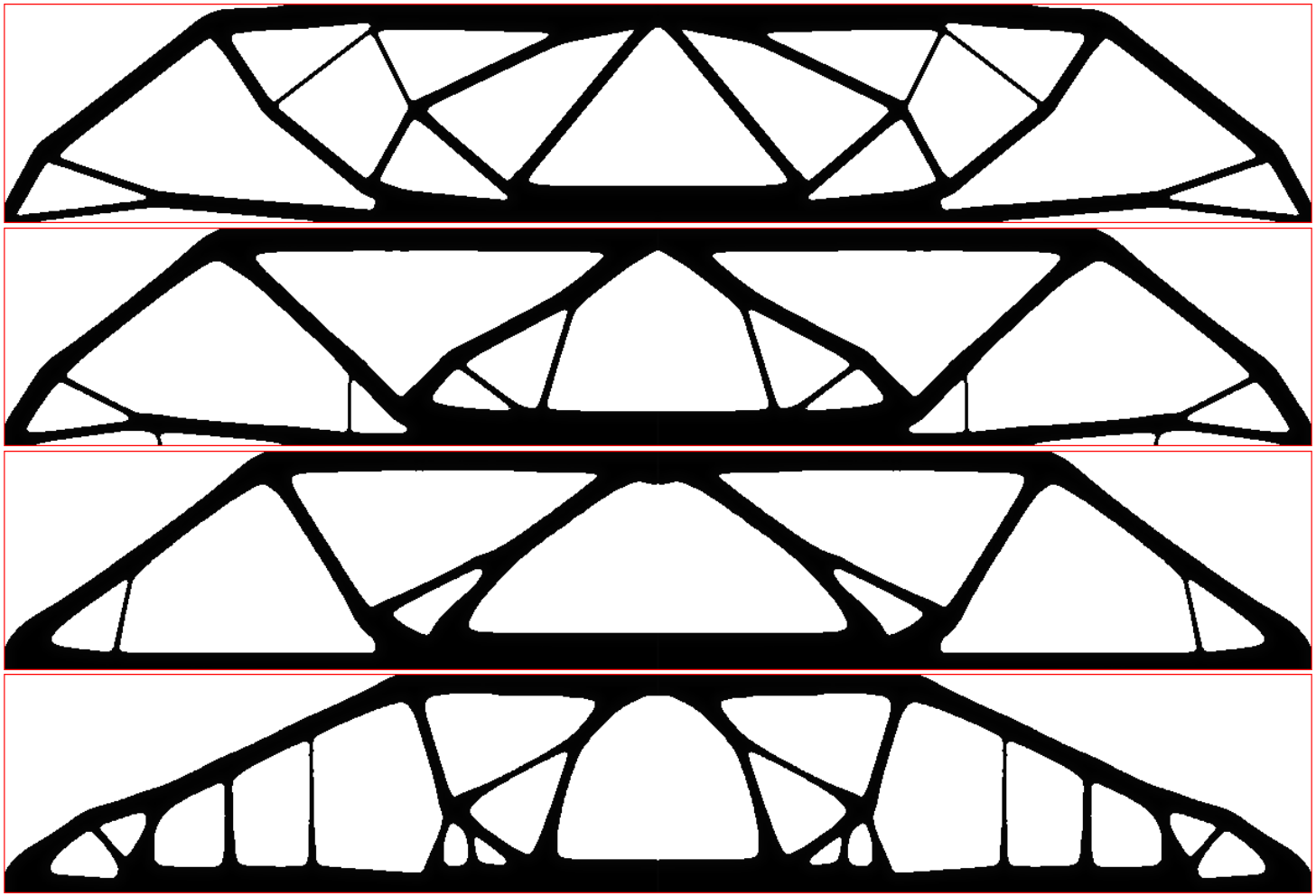

Optimized shapes for the two-dimensional MBB Beam example; (top) optimized shape Ω^**, without additive manufacturing constraints, and optimized shapes using parameters (from top to bottom)* $\alpha_c = 0.50$*,* $\alpha_c = 0.30$*, and* $\alpha_c = 0.10$*.*

Mechanical approach: the manufacturing compliance (III)

This new approach yields better results; yet, it raises two issues:

1. $P_{\mathrm{sw}}(\Omega)$ inherently favors structures whose lower part is stronger.
2. The optimized shapes still show large, completely horizontal overhangs. This is a flaw in the modelling of $P_{\mathrm{sw}}(\Omega)$, which assumes that each layer of material is assembled instantaneously.

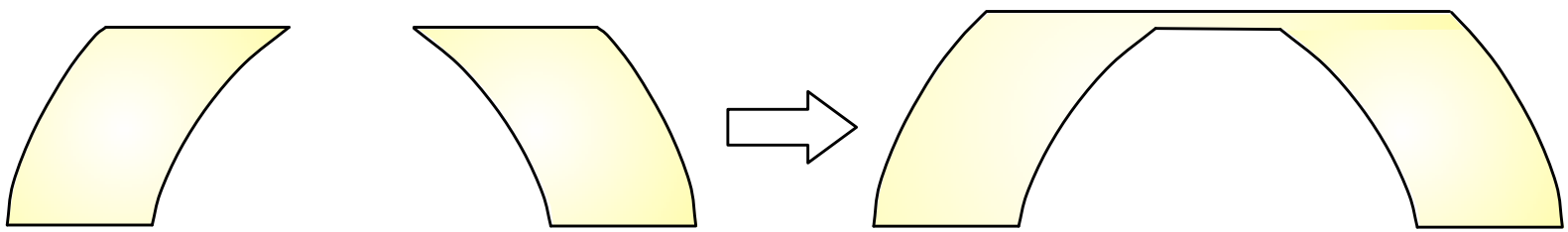

Completely flat overhangs are not so weak because of the instantaneous layer deposition assumption.

Mechanical approach: the modified manufacturing compliance (I)

We now solve:

$$\begin{array}{ll} \min\limits_{\Omega} & J(\Omega) \\ \text{s.t.} & \mathrm{Vol}(\Omega) \leq \alpha_v \mathrm{Vol}(D), \\ & P_{\mathrm{uw}}(\Omega) \leq \alpha_c P_{\mathrm{uw}}(\Omega^*), \end{array}$$

where the modified (upper weight) manufacturing compliance $P_{\mathrm{uw}}(\Omega)$ brings into plays elastic displacements of the intermediate shapes $u^a_{\Omega_h}$ involving an artificial load concentrated on their upper side:

$$\begin{cases} -\mathrm{div}(Ae(u^a_{\Omega_h})) = g_h & \text{in } \Omega_h, \\ u^a_{\Omega_h} = 0 & \text{on } \Gamma_0, \\ Ae(u^a_{\Omega_h})n = 0 & \text{on } \Gamma^l_h, \\ Ae(u^a_{\Omega_h})n = 0 & \text{on } \Gamma^u_h, \end{cases} \quad \text{where } g_h(x) = \begin{cases} g & \text{if } x_d \in (h-\delta, h), \\ 0 & \text{otherwise.} \end{cases}$$

Mechanical approach: the modified manufacturing compliance (II)

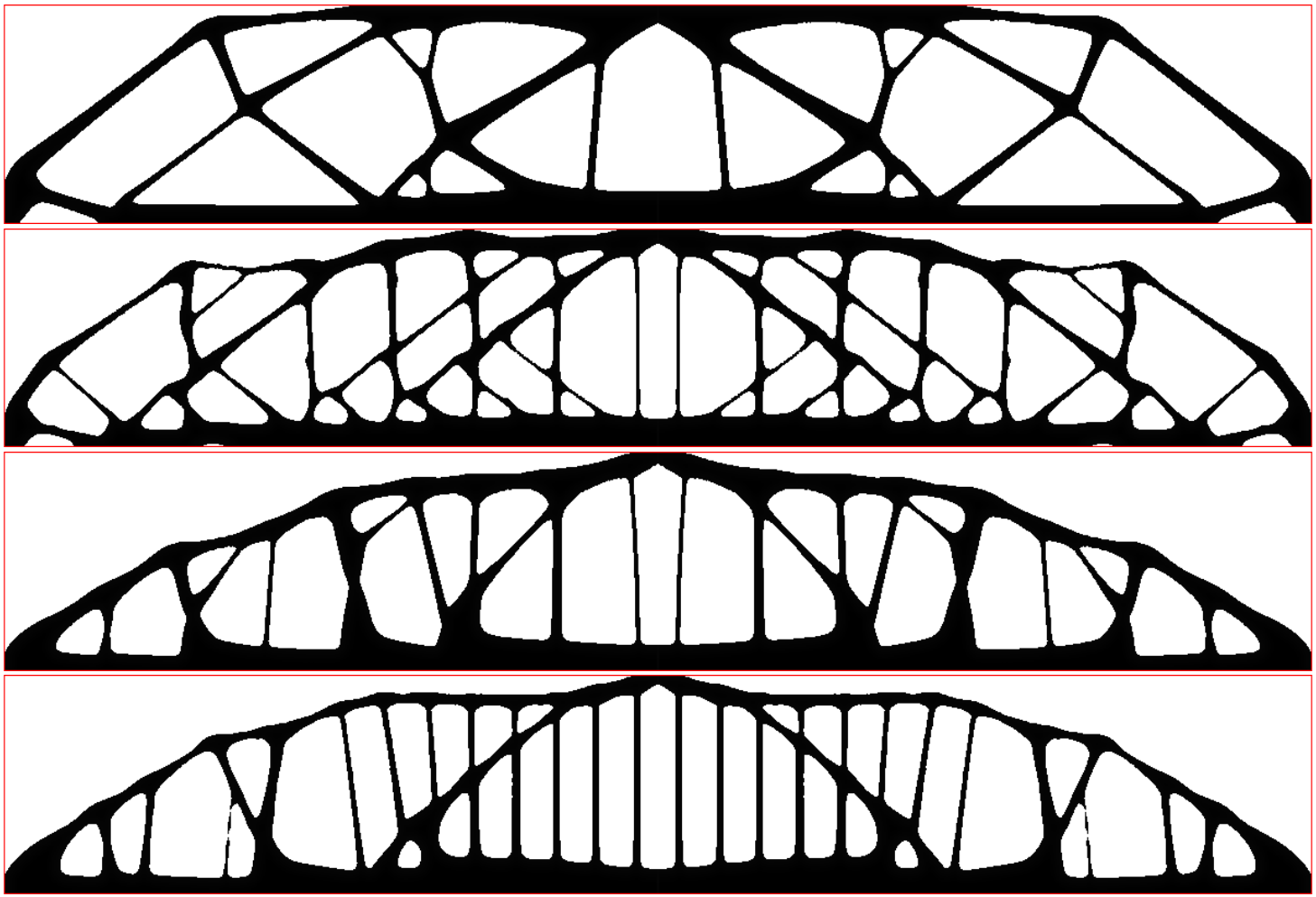

Optimized 2d MBB Beams obtained using the modified manufacturing compliance $P_{\mathrm{af}}(\Omega)$ *and parameters (from top to bottom)* $\alpha_c = 0.30$, $\alpha_c = 0.10$, $\alpha_c = 0.05$, *and* $\alpha_c = 0.03$.

Mechanical approach: the modified manufacturing compliance (III)

We now consider the design of a three-dimensional bridge.

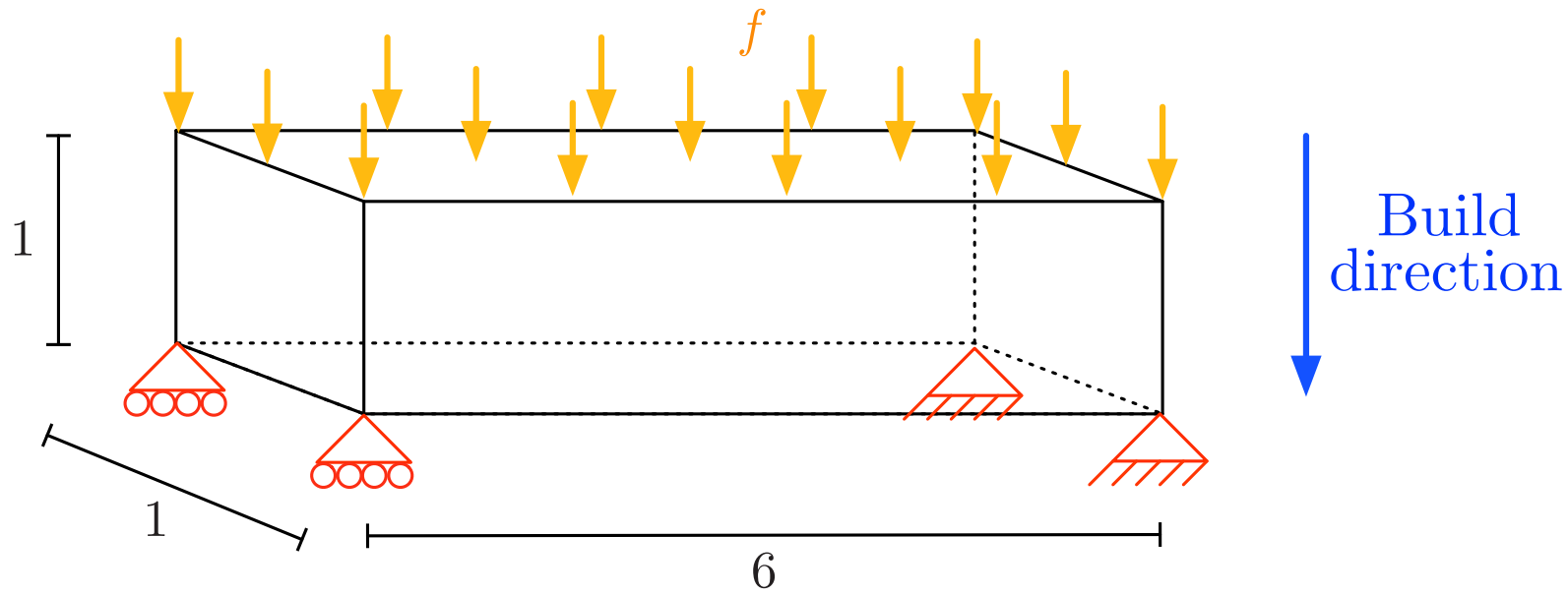

We solve the following shape optimization problem:

$$\begin{aligned} \min_{\Omega} \quad & \mathrm{Vol}(\Omega), \\ \text{s.t.} \quad & J(\Omega) \leq J(\Omega^*), \\ & P_{\mathrm{uw}}(\Omega) \leq \alpha_c P_{\mathrm{uw}}(\Omega^*). \end{aligned}$$

Mechanical approach: the modified manufacturing compliance (IV)

The optimized shape Ω^* without manufacturing shows several large overhangs.

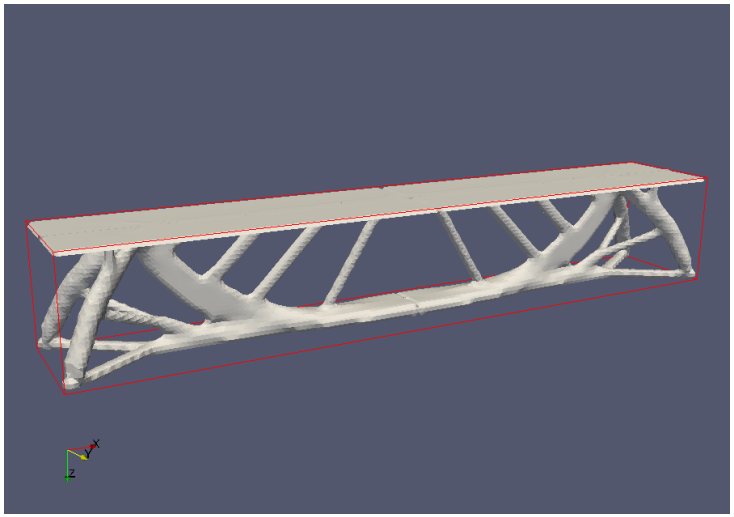

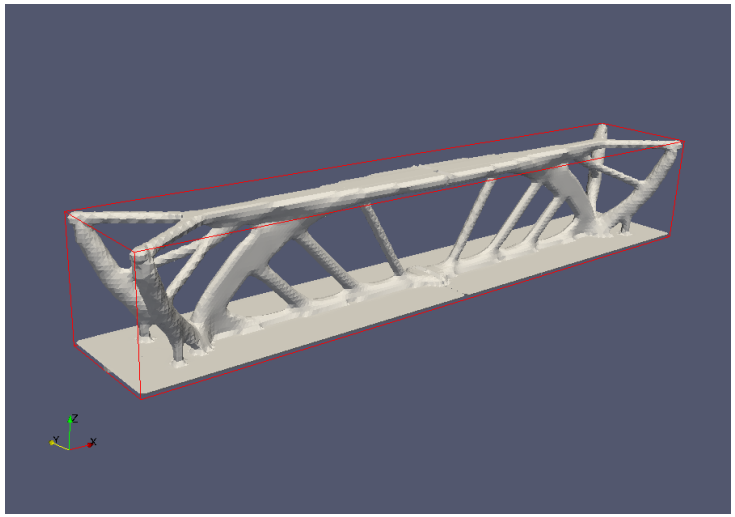

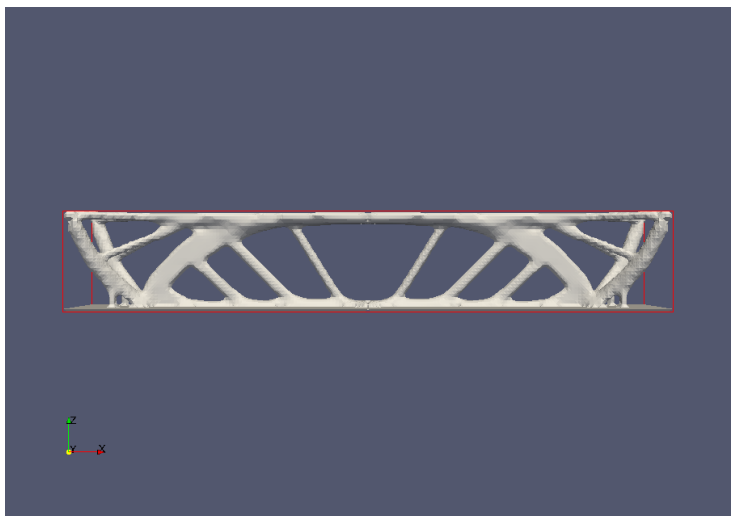

Different views of the unconstrained optimized shape Ω^*.

Mechanical approach: the modified manufacturing compliance (V)

Several small overhangs remain on the upper part of the optimized shape with the imposed manufacturing constraint $P_{\mathrm{uw}}(\Omega)$.

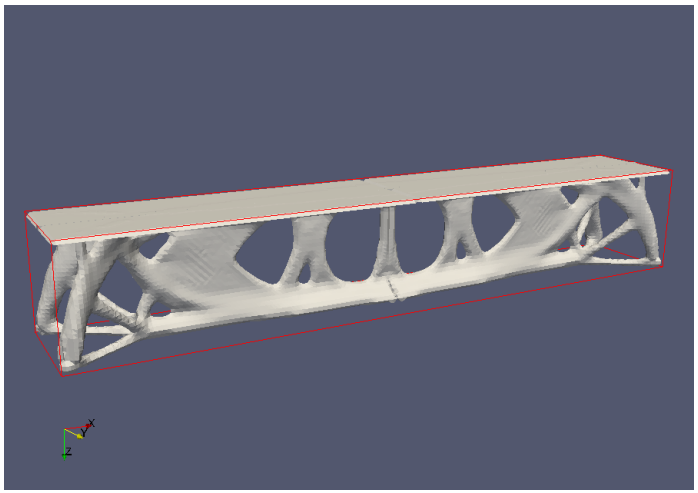

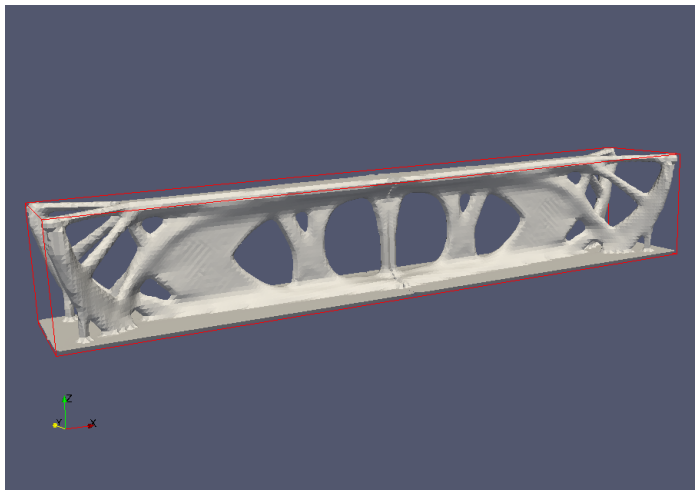

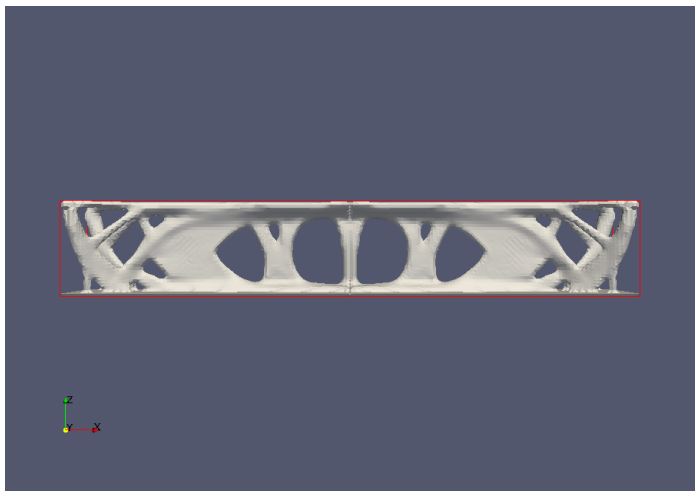

Different views of the optimized shape for $\alpha_c = 0.1$.

1. Additive manufacturing techniques: assets and drawbacks
   - Additive manufacturing in a nutshell
   - The overhang issue
2. The shape optimization problem
3. Geometric constraints for the presence of overhangs
   - The 'naive', geometric attempt
   - Insufficiency of the geometric constraints
4. Geometric constraints for the presence of overhangs
   - Presentation of the mechanical constraint
   - Shape derivative of the mechanical constraint
   - Other models
5. Numerical evaluation of $P_{\mathrm{sw}}(\Omega)$ and its derivative
6. Numerical examples
   - Test of the mechanical approaches
   - Combining the geometric and mechanical approaches

Mixing geometric and mechanical formulations (I)

To remedy these completely flat regions caused by the instantaneous layer deposition, we consider the following optimization problem, which mixes geometric and mechanical constraints:

$$\begin{aligned} \min_{\Omega} \quad & (1-\alpha_g)\frac{\mathrm{Vol}(\Omega)}{\mathrm{Vol}(\Omega^*)} + \alpha_g \frac{P_g(\Omega)}{P_g(\Omega^*)}, \\ \text{s.t.} \quad & J(\Omega) \leq J(\Omega^*). \\ & P_{\mathrm{uw}}(\Omega) \leq \alpha_c P_{\mathrm{uw}}(\Omega^*). \end{aligned}$$

Mixing geometric and mechanical formulations (II)

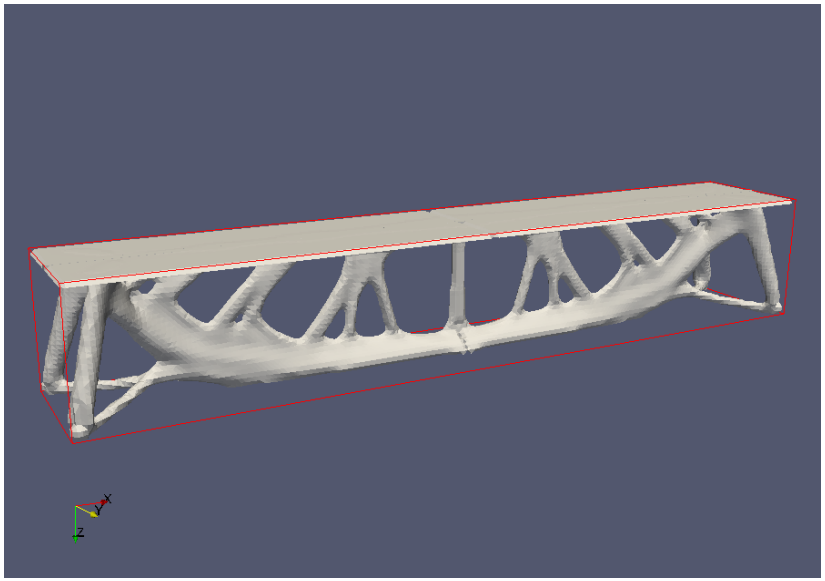

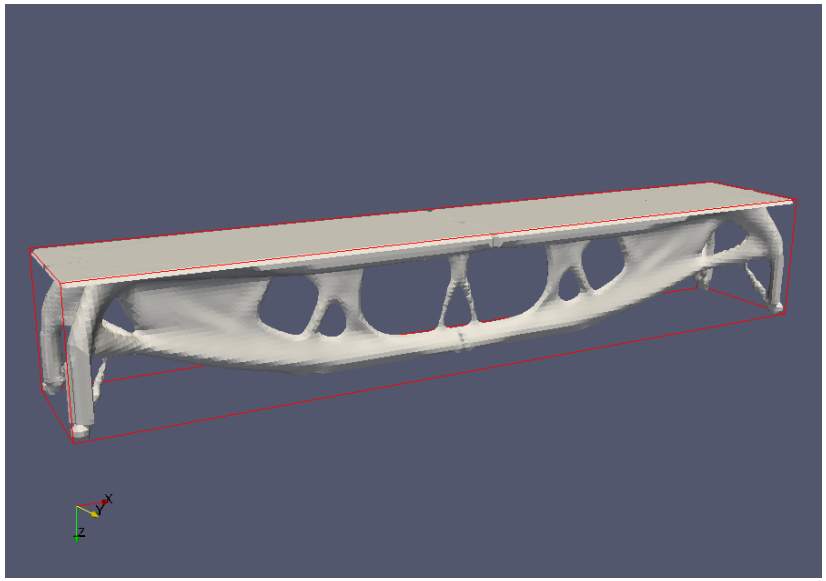

Optimized 3d bridges for the combined geometrically and mechanically constrained problem, setting (left) $\alpha_c = 0.10$, $\alpha_g = 0.10$, *and (right)* $\alpha_c = 0.10$, $\alpha_g = 0.90$.

Mixing geometric and mechanical formulations (III)

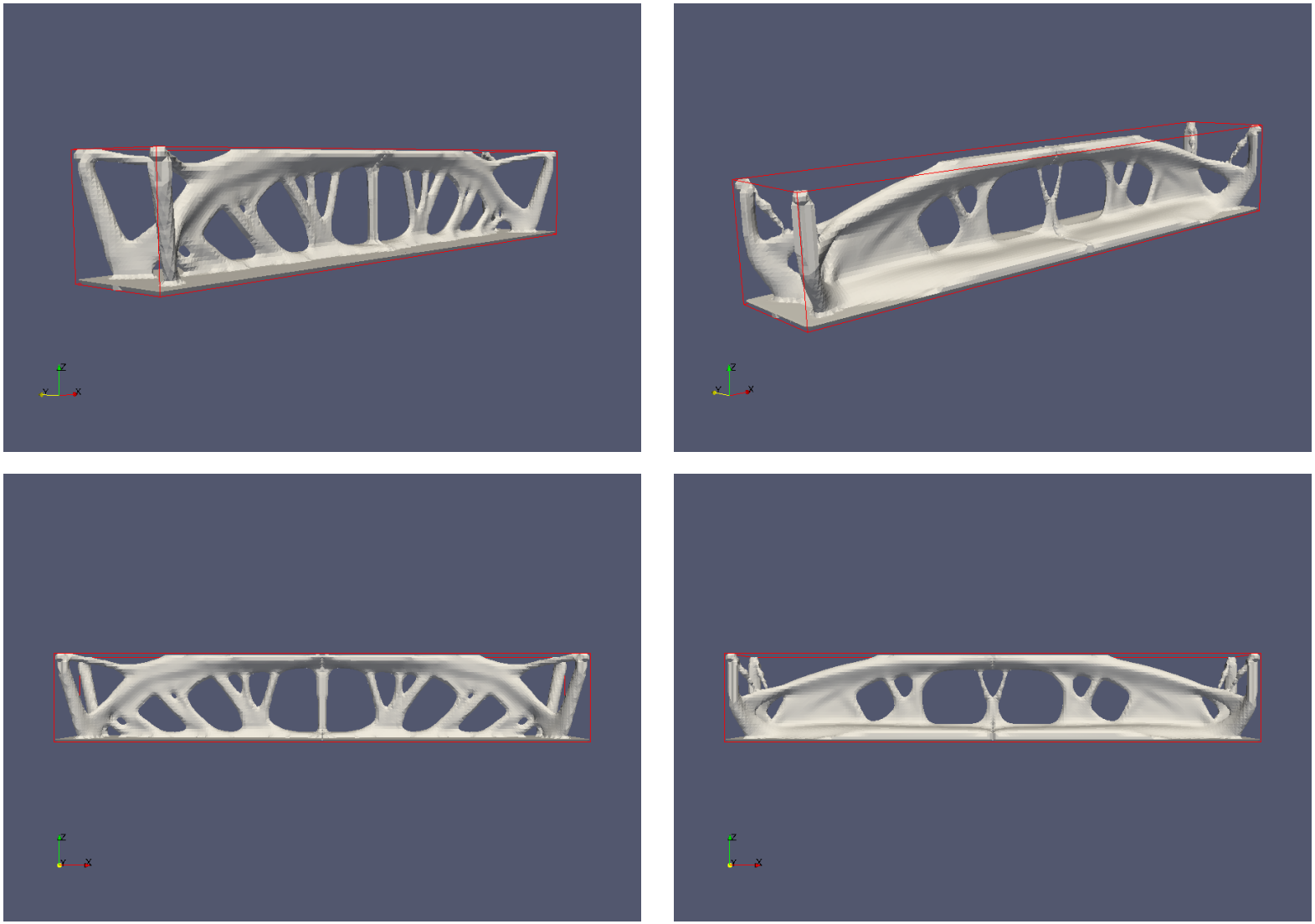

Different views of the optimized shapes with (left) $\alpha_c = 0.10$, $\alpha_g = 0.10$, *and (right)* $\alpha_c = 0.10$, $\alpha_g = 0.90$.

Thank you !

Thank you for your attention!

References I

[AlJak] G. Allaire, L. Jakabcin, *Taking into account thermal residual stresses in topology optimization of structures built by additive manufacturing*, (in preparation).

[AlDaFauMiEs] G. Allaire, C. Dapogny, A. Faure, G. Michailidis and R. Estevez, *Shape optimization of a layer by layer mechanical constraint for additive manufacturing*, accepted for publication in C. R. Math. Acad. Sci. Paris. HAL preprint: hal-01398877 (2016).

[AlDaFauMiEs2] G. Allaire, C. Dapogny, A. Faure, G. Michailidis and R. Estevez, *Structural optimization under overhang constraints imposed by additive manufacturing technologies*, submitted, (2017).

[CheLuChou] B. Cheng, P. Lu and K. Chou, *Thermomechanical Investigation of Overhang Fabrications In Electron Beam Additive Manufacturing*, ASME 2014 International Manufacturing Science and Engineering Conference, (2014).

[DuHeLe] J. Dumas, J. Hergel and S. Lefebvre, *Bridging the Gap: Automated Steady Scaffoldings for 3D Printing*, ACM Trans. Graph., 33, 4, (2014), pp. 1–10.

References II

[GiRoStu] I. Gibson, D.W. Rosen and B. Stucker, *Additive manufacturing technology: rapid prototyping to direct digital manufacturing*, Springer Science Business Media, Inc, (2010).